Analytical Methods

PAPER

View Article Online
View Journal | View Issue

Cite this: *Anal. Methods*, 2014, **6**, 1684

A sensitive HPLC assay for quantitative determination of polyamidoamine dendrimers after pre-column derivatization using FITC

Zhou Jiang,[b] Jina Yang,[a] Rui Wang[a] and Jian Wang*[a]

Received 27th October 2013
Accepted 6th January 2014

DOI: 10.1039/c3ay41896k

www.rsc.org/methods

A pre-column derivatization method was developed to analyze polyamidoamine (PAMAM) dendrimers. The fluorescein isothiocyanate (FITC) derivation method improved the retention of PAMAM dendrimers on the reversed-phase column of high performance liquid chromatography (RP-HPLC). The derivation benefited the UV-Vis detection of PAMAM, although the fluorescence of FITC was quenched by PAMAM dendrimers. The primary amine-terminated PAMAM dendrimers, generation 3 (PAMAM-NH_2 (G3)), were quantitatively determined by UV-Vis spectroscopy over the concentration range of 10–80 μg mL^{-1}, with the calibration curve expressed as $A = 131.6C$ (μg mL^{-1}) − 295.6 ($R^2 = 0.9901$) and the detection limit of 2.7 μg mL^{-1}. The binding ratio of FITC to PAMAM-NH_2 (G3) was determined as 8 : 1 by liquid chromatography-electrospray ionization-ion trap mass spectrometry (LC-ESI-IT-MS).

1. Introduction

Dendrimers are globular nano-structure macromolecules, which consist of a central core emanating repetitively branched arms. There are a large number of functional groups on the surface which can be modified to bring about special physical and chemical properties.[1,2] Accordingly, dendrimers have attracted increasing attention for their applications in various fields such as drug delivery systems.[3–5] Compared with conventional macromolecules, polyamidoamine (PAMAM)-NH_2 has much higher amino group density, and can bind drug molecules on the surface. Besides, they possess empty internal cavities in which drug molecules can be easily encapsulated. Thus, PAMAM-NH_2 is a potential drug carrier, especially for hydrophobic drugs.[4,5] In addition, the nano-structure also favorite this application by enhancing the drug bioavailability and biodistribution, and possibly by taking advantage of the enhanced permeation and retention (EPR) effect for targeting tumors.[6]

Various techniques have been utilized to analyze PAMAM dendrimers and their derivatives, including but not limited to NMR spectroscopy,[7,8] matrix-assisted laser desorption ionization-time of flight (MALDI-TOF) mass spectrometry,[9,10] and capillary electrophoresis (CE).[11–15] HPLC has been utilized to separate and characterize various PAMAM dendrimers or conjugates,[16] to evaluate the polydispersity, surface heterogeneity, and solubility of multi-functionalized dendrimers,[17] as well as to study the interactions between biomolecules and dendrimers.[18] Although HPLC provides critical technical support for pharmacokinetics studies, its application in PAMAM dendrimers is restricted owing to the weak absorption in the UV region (less than 210 nm) and the poor retention on the conventional RP-HPLC column. Current HPLC analysis for PAMAM dendrimers commonly requires a special RP column (such as C5 column) and complex mobile phase with a limit of detection (LOD) of 1000 μg mL^{-1} or higher.[19,20]

Therefore, we herein reported a more sensitive HPLC method for analyzing PAMAM by pre-column derivatization with fluorescein isothiocyanate (FITC). Moreover, liquid chromatography-electrospray ionization-ion trap mass spectrometry (LC-ESI-IT-MS) was used to analyze the binding ratio of FITC to PAMAM dendrimers. The findings not only improve the analytical capability of HPLC for PAMAM dendrimers, but also provide valuable information regarding their characteristics.

2. Experimental

2.1 Materials

Amine terminated PAMAM dendrimer with ethylenediamine core, generation 3 (PAMAM-NH_2 (G3) dendrimer, molecular weight: 6909 Da), was purchased from Dendritech (>95%, Weihai CY Dendrimer Technology Co., Ltd.). FITC was obtained from Sigma-Aldrich (America). Ultra-pure water (18.2 MΩ cm^{-1}) prepared with a Suken purification system (Kertone Ltd.) was used throughout the experiments. Other reagents were analytically pure.

[a]*Ministry of Education Key Laboratory of Analysis and Detection for Food Safety, Fujian Provincial Key Laboratory of Analysis and Detection for Food Safety, Fuzhou University, Fuzhou, Fujian 350108, China. E-mail: jwang@fzu.edu.cn*

[b]*Institute of Research on Functional Materials, Cancer Metastasis Alert and Prevention Center, College of Chemistry and Chemical Engineering, Fuzhou University, Fuzhou, Fujian 350108, China*

2.2 Derivation procedures

Stock solutions (0.2 mg mL^{-1}) of PAMAM-NH_2 (G3) dendrimers were prepared with acetonitrile (ACN). Stock solutions of FITC (1 mg mL^{-1}) were prepared by dissolution in acetone and stored at 4 °C before use.

An aliquot of 200 μL FITC stock solution was added to 5 weighing bottles, respectively. When the solvent completely volatilized, 150 μL, 300 μL, 600 μL, 900 μL and 1200 μL of PAMAM-NH_2 (G3) dendrimer stock solutions were added respectively and diluted to 3 mL with ACN. The reaction solutions were continuously stirred for 12 h in the dark, and then used directly for HPLC and LC-MS analyses.

2.3 Instruments

A Lambda 750 UV-Vis spectrometer (Japan) and an Eclipse fluorescence spectrophotometer (Varian, America) were used to detect the derivatives.

The reversed-phase HPLC system consists of dual pumps, a SIL-20AT autosampler, a CTO-10ASvp thermostat and a SPD-20AV UV detector (Shimadzu, Japan). The VP-ODS C18 analytical column (250 mm × 4.6 mm, 5 μm) was purchased from Shimadzu (Tokyo, Japan). The procedure elution was usually a linear gradient beginning with 5% ACN to 95% ACN in 15 min and hold at 5% water/95% ACN to 25.0 min. Unless specified, the injection volume was 20 μL, the detection wavelength was set at 455 nm, and the column temperature was set at 36 °C.

LC-MS analyses were performed with an LCQ Fleet ion trap mass spectrometer (IT-MS^n) (Thermo Fisher Scientific) in positive electrospray mode. Across the 50–2000 *m*/*z* range, all scan events were acquired with a 200 ms maximum ionization time. The ion source-dependent parameters were optimized as: electrospray voltage, 4.5 kV; capillary temperature, 350 °C; sheath gas flow rate, 35 units; aux gas flow rate, 5 units; I spray voltage, 4.00 kV; tube lens, 60 V. Data were obtained and processed with Xcalibur 1.2 and LC Quan 2.0 SP1 software. The IT-MS system was calibrated with a 1 pg μL^{-1} reserpine solution through an automated instrument calibration.

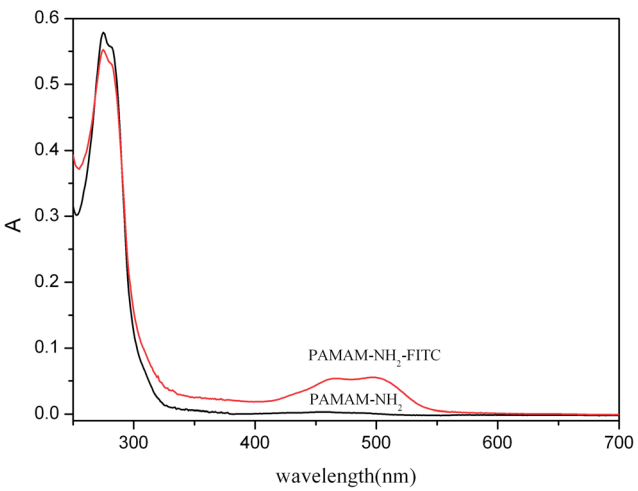

Fig. 1 UV-Vis absorption spectra of PAMAM-NH_2 (G3) and PAMAM-NH_2 (G3)–FITC derivative in phosphate buffer. FITC: 1.72 × 10^{-4} mol L^{-1}, PAMAM-NH_2: 80 ppm.

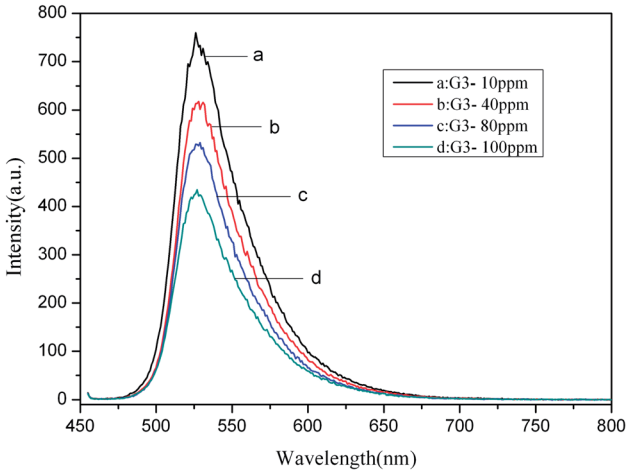

Fig. 2 Fluorescence emission spectra (excitation wavelength: 450 nm, scanning range: 455–800 nm) of PAMAM-NH_2 (G3)–FITC derivative with different amounts of additional PAMAM-NH_2 (G3).

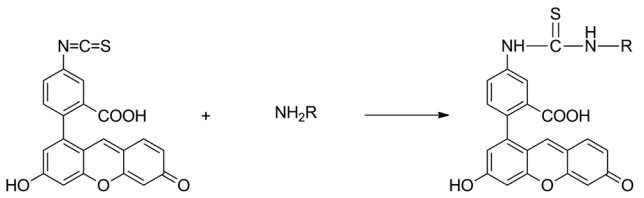

Scheme 1 Derivatization of the PAMAM-NH_2 (G3) dendrimer with FITC.

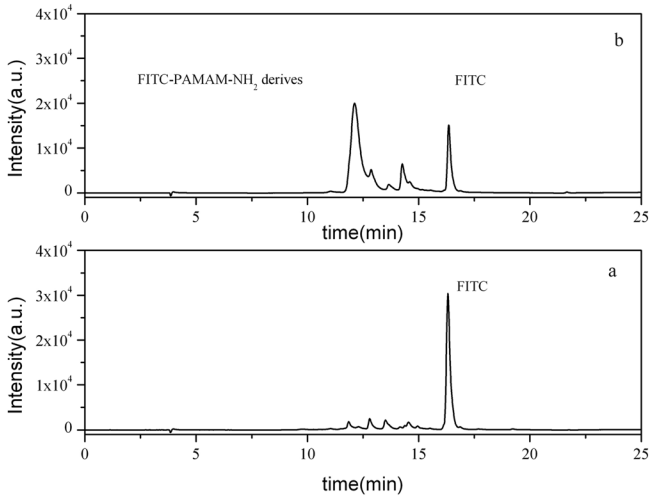

Fig. 3 Chromatograms of FITC (a) and PAMAM-NH_2 (G3)–FITC derivative (b). The flow rate was 1 mL min^{-1}. Gradient: A, water, B, ACN, 0–15 min, 5–95% B; 15–25 min, hold at 95% B. The wavelength of maximum absorbance was 455 nm.

The HPLC system was equipped with a thermostatted autosampler Accela autosampler (Thermo Fleet), a quaternary pump (Thermo Fleet), and a diode array Accela PDA detector (Thermo Fleet). LC analysis was performed with a reversed-phase C18 analytical column (Venusil XBP, 100 mm × 2.1 mm, 3 μm, Agela). Mobile phases A and B were water and ACN with 0.1% formic acid in both phases. The flow rate was 200 μL min^{-1}. A linear gradient was set from 5% to 95% of B in 15 min and hold at 5% water/95% ACN to 25.0 min. The injection volume was 20 μL. Xcalibur (1.2) software was used to evaluate the collected data.

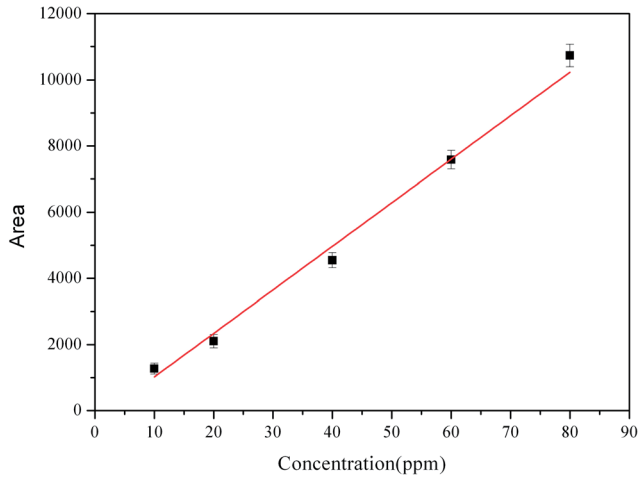

Fig. 4 Calibration curve of the PAMAM-NH_2 (G3) dendrimer.

3. Results and discussion

3.1 Characterization of the interaction between PAMAM-NH_2 (G3) dendrimers and FITC: fluorescence and UV-Vis spectrophotometry

In Fig. 1, curve a is the UV-Vis absorption spectrum of PAMAM-NH_2 (G3) in PBS against pure water as blank. Actually, the weak absorption of PAMAM-NH_2 (G3) in the UV region fades in the background absorption of PBS centered at around 275 nm. In contrast, the FITC derivative has a broad visible absorption over 400–550 nm, with the peak at 455 nm (Fig. 1, curve b). Despite FITC is a good fluorescent agent, the fluorescence of PAMAM-NH_2 (G3)–FITC cannot be well detected. As shown in Fig. 2, with increasing concentration of PAMAM-NH_2 (G3), the fluorescence intensity of the mixture excited at 455 nm declines gradually, indicating that PAMAM-NH_2 (G3) dendrimers quenched the

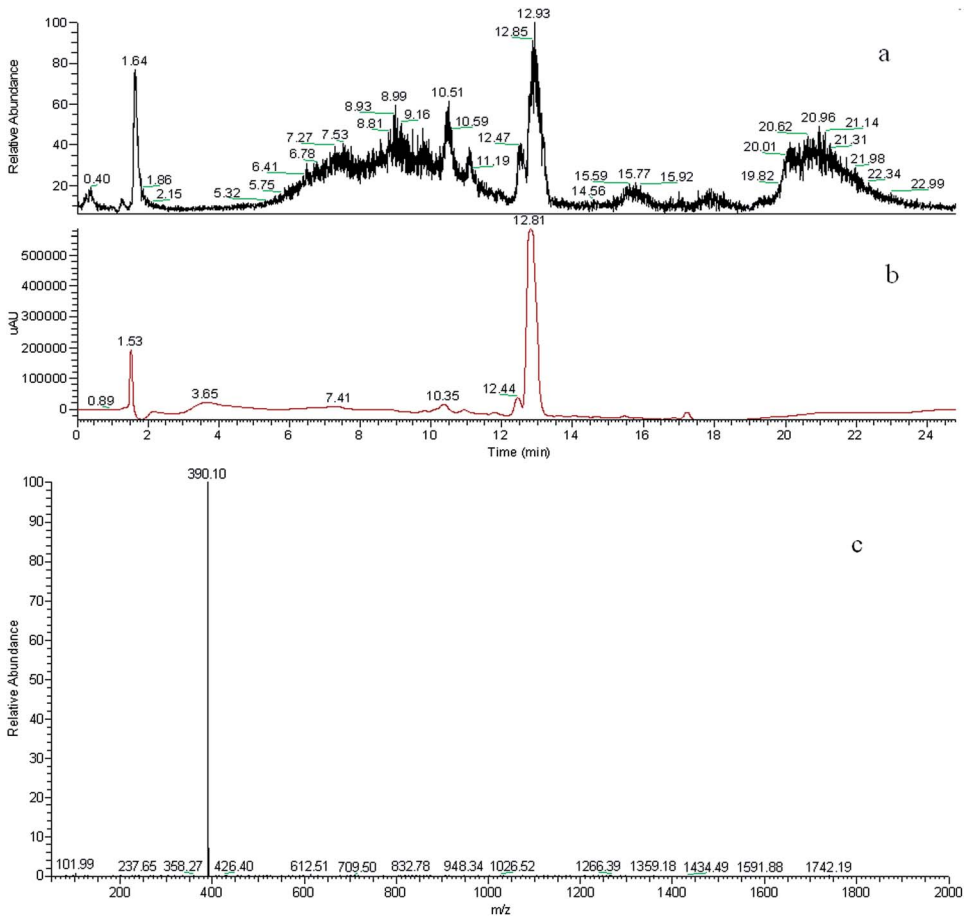

Fig. 5 LC-MS analyses of FITC. (a) Total ion chromatography. (b) PDA chromatogram. (c) ESI-MS spectrum (positive mode) of FITC. Mobile phases: water (A) and ACN (B) with 0.1% formic acid in both phases. Gradient: A, water, B, ACN, 0–15 min, 5–95% B; 15–25 min, hold at 95% B, and the flow rate was 0.2 mL min^{-1}.

fluorescence of FITC. Thus, the fluorescence detection was not suitable for the mixture. Instead, UV detection was adopted.

3.2 HPLC analysis

PAMAM-NH_2 (G3) dendrimers perform poor retention in the C18 column owing to the extremely strong polarity (hydrophilicity), which was circumvented by the derivatization method. Multiple amino groups of dendrimers are prone to react with the sulfur cyanide group of FITC under certain conditions (Scheme 1). Excess FITC was added to completely transform PAMAM-NH_2 (G3). The hydrophobicity of PAMAM-NH_2 (G3)–FITC derivatives depended primarily on the surface density of the rest of the primary amine groups.

Fig. 3 shows the HPLC chromatograms of FITC (Fig. 3a) and the resulting mixture after derivatization (Fig. 3b). Since excess

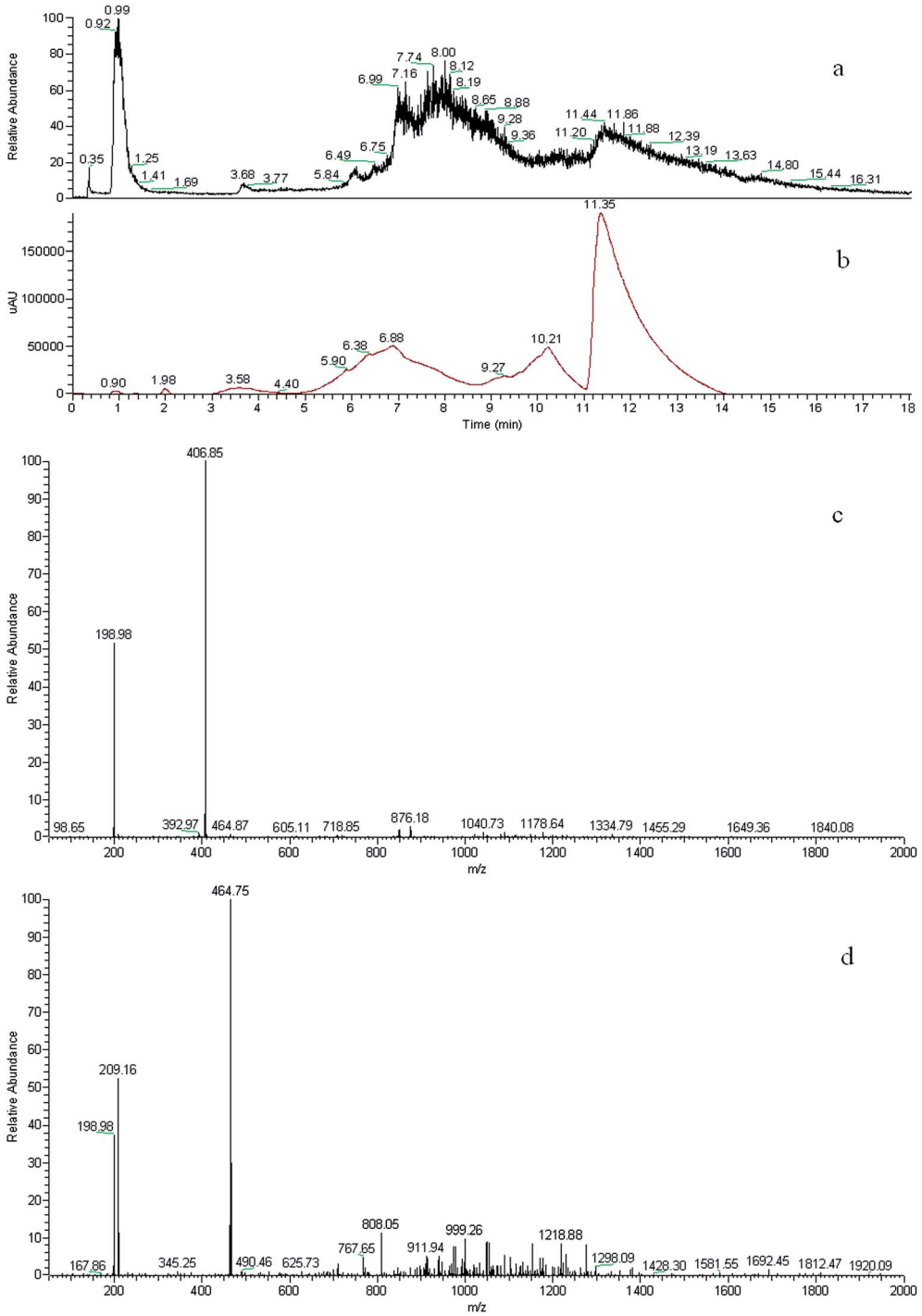

Fig. 6 LC-MS analyses of PAMAM-NH_2 (G3). (a) Total ion chromatography. (b) PDA chromatogram. (c and d) ESI-MS spectrum (positive mode) of FITC at 11.44 min and 10.18 min, respectively. The same LC conditions are given in Fig. 5.

FITC was added, there were two main peaks in the chromatograph of derivatives. With increasing concentration of PAMAM-NH_2 (G3) dendrimers, the peak intensity at 16.9 min slightly reduced. In contrast, the peak at 12.4 min obviously enhanced. Obviously, the peaks at 12.4 min and 16.9 min correspond to the PAMAM-NH_2 (G3)–FITC derivatives and FITC respectively. The calibration curve of PAMAM-NH_2 (G3) dendrimers was shown in Fig. 4, which can be expressed as $A = 131.6C\ (\mu g\ mL^{-1}) - 295.6$, $R^2 = 0.9901$ over the concentration range from 10 to 80 $\mu g\ mL^{-1}$.

The binding ratio of derivatives was determined by comparing the increase of PAMAM-NH_2 (G3) concentration with the decrease of FITC concentration. The absolute concentration of FITC was 1.72×10^{-4} mol L^{-1}, and the concentration of PAMAM-NH_2 (G3) increased from 10 $\mu g\ mL^{-1}$ (1.4×10^{-6} mol L^{-1}) to 80 $\mu g\ mL^{-1}$ (11.2×10^{-6} mol L^{-1}).

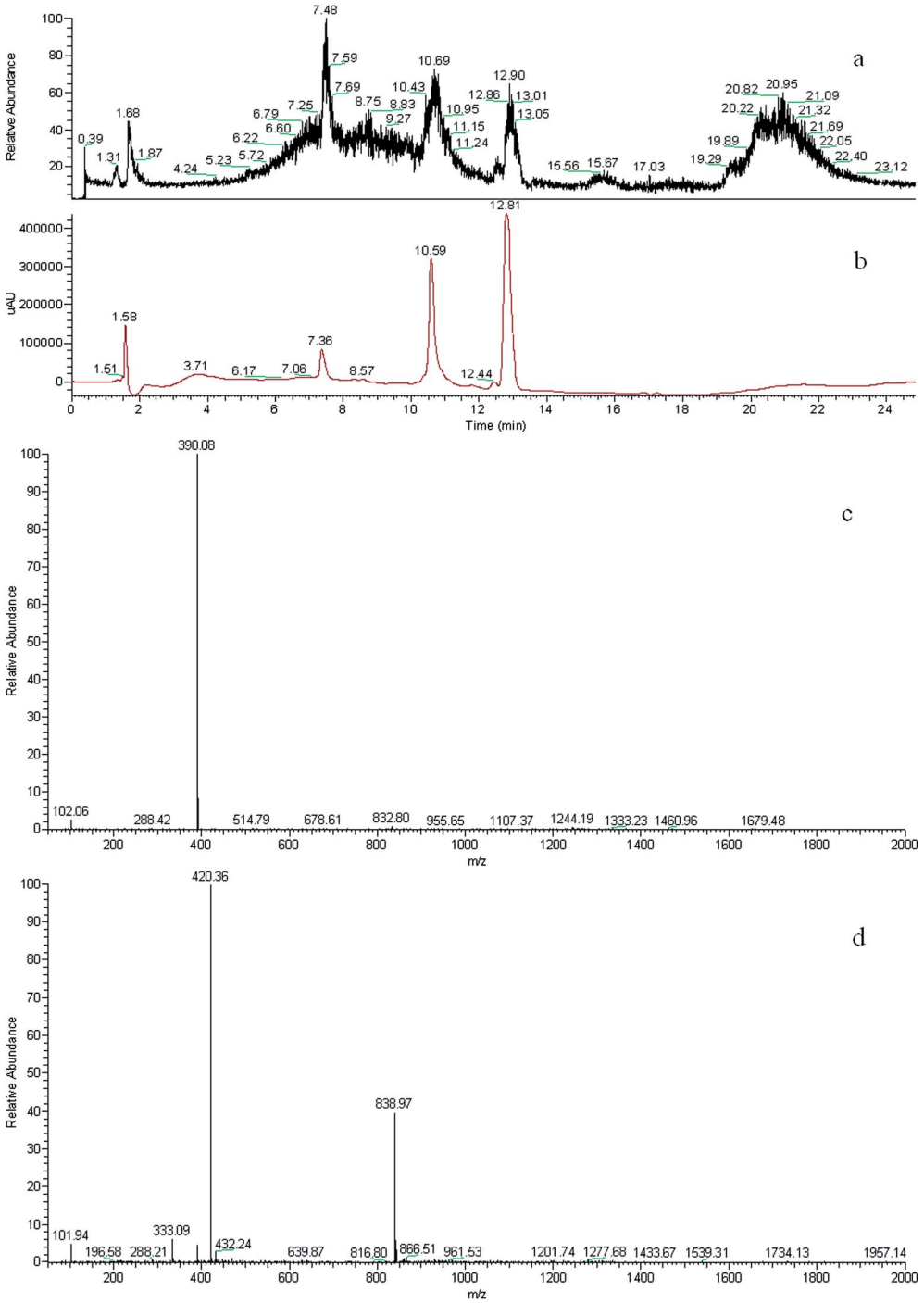

Fig. 7 LC-MS analyses of PAMAM-NH_2 (G3)–FITC. (a) Total ion chromatography. (b) PDA chromatogram. (c and d) ESI-MS spectrum of PAMAM-NH_2 (G3)–FITC at 12.81 min and 10.59 min, respectively. The same LC conditions are given in Fig. 5.

The derivation formula is expressed as follows:

$$n = \frac{\Delta C_{\mathrm{FITC}}}{\Delta C_{\mathrm{PAMAM}}} = \frac{(A_{10\ \mathrm{ppm}} - A_{80\ \mathrm{ppm}})/A_{10\ \mathrm{ppm}} \times C_{\mathrm{FITC}}}{C_{80\ \mathrm{ppm}} - C_{10\ \mathrm{ppm}}}$$
$$= \frac{(7226.4 - 3959.3)/7226.4 \times 1.72 \times 10^{-4}}{11.2 \times 10^{-6} - 1.4 \times 10^{-6}} = 7.935$$

Therefore, the binding ratio of FITC to PAMAM-NH_2 (G3) dendrimer was determined to be 8 : 1.

3.3 LC-MS analysis

PAMAM-NH_2 (G3) is a symmetrical molecule that contains 32 surface groups of primary amine. Thus it readily generates multiply charged ions during ESI detection due to considerable proton affinity. As mentioned above, a PAMAM-NH_2 (G3) can bind 8 FITC and leave many amine groups excessive. Hence, PAMAM-NH_2 (G3)–FITC can also be ionized by ESI in the form of $[M + zH]^{z+}$.

Fig. 5 shows the LC-MS spectrogram of FITC. From the total ion chromatography (TIC) (Fig. 5a), FITC had an extremely high response intensity, suggesting that FITC was appropriate for ESI ionization. The main peak (12.81 min) in the selected-ion monitoring (SIM) chromatogram (Fig. 5b) at *m*/*z* 390.10 (Fig. 5c) represents protonated FITC whose theoretical *m*/*z* value is 390.38 ($[M_{\mathrm{FITC}} + M_{\mathrm{H}}]^{+}$).

The LC-MS spectrogram of PAMAM-NH_2 (G3) dendrimers is shown in Fig. 6. The peak at *m*/*z* 198.98 (Fig. 6c) is assigned to $[M_{G3} + 35M_{H}]^{35+}$. Since there are only 32 primary amine groups on the molecular surface, some secondary amine groups might be ionized within the molecule. $[M_{G3} + 17M_{H}]^{17+}$ ions were produced because the PAMAM-NH_2 (G3) dendrimer obtained 17 hydrogen ions, verifying the signal at *m*/*z* 406.85 at 11.44 min (Fig. 6c). A multi-charged sodium adduct $[M_{G3} + 2M_{Na} + 13M_{H}]^{15+}$ appeared at *m*/*z* 464.75 at 10.18 min as the dominant signal (Fig. 6d), and the sodium ions originated from random Na impurity. Meanwhile, there were two relatively low-intensity signals, *i.e.* $[M_{G3} + 33M_{H}]^{33+}$ and $[M_{G3} + 35M_{H}]^{35+}$, at *m*/*z* 209.16 and 198.98 (Fig. 6d).

As exhibited in Fig. 7, two higher peaks appear after derivatization (Fig. 7b), with the retention times of 12.81 min and 10.59 min, respectively. The peak at 12.81 min (Fig. 7b and c) can be assigned to FITC. Fig. 7d presents that $[M_{G3} + xM_{FITC} + (32 - x)M_{H}]^{32-x}$ emerges at *m*/*z* 420.36. Presumably, a part of terminal amino groups bound to FITC and the rest were protonated, based on which the binding ratio was estimated to be 8. The form corresponds to the *m*/*z* values of $(M_{G3} + 8M_{FITC} + 24M_{H})/24$. However, the signal of *m*/*z* 838.97 cannot be ascribed to $[M_{G3} + xM_{FITC} + (32 - x)M_{H}]^{32-x}$ because amide was so weakly nucleophilic that the reaction with FITC was impossible. Hence, the peak at *m*/*z* 838.97 can be assigned to $(2(M_{G3} + 8M_{FITC}) + 24M_{H})/24$, *i.e.* the derivative dimer.

4. Conclusions

In summary, PAMAM dendrimers were converted to derivatives, which could be highly selectively detected by HPLC. This derivatization method, which was successfully applied to determine the standards, may be useful for biomedical and clinical investigations. In addition, the LC-MS study is feasibly applicable to in-depth analysis of the derivatives.

Acknowledgements

This research was supported by the National Natural Sciences Foundation of China (Grant no. 81273548), the Foundation of the Education Department of Fujian Province, China (JK2010003) and the Scientific and Technological Foundation of Fujian Province of China (2011J01043).

References

1 D. A. Tomalia, H. Baker and J. Dewald, A new class of polymers: starburst dendritic macromolecules, *Polym. J.*, 1985, **17**, 117–132.
2 D. A. Tomalia and J. R. Dewald, Dense star polymers having two dimensional molecular diameter, *U.S. Pat.*, 4587329, 1986.
3 A. Choksi, K. V. L. Sarojini, P. Vadnal, *et al.*, Comparative antiinflammatory activity of poly(amidoamine) (PAMAM) dendrimer–dexamethasone conjugates with dexamethasone-liposomes, *Int. J. Pharm.*, 2013, **449**, 28–36.
4 R. G. Elizabeth and J. M. J. Fréchet, Dendrimer and dendritic polymers in drug delivery, *Drug Discovery Today*, 2005, **10**, 35–43.
5 R. Esfand and D. A. Tomalia, Polyamidoamine (PAMAM) dendrimer: from biomimicry to drug delivery and biomedical applications, *Drug Discovery Today*, 2001, **6**, 427–436.
6 F. E. Koç and M. Şenel, Solubility Enhancement of Non-Steroidal Anti-Inflammatory Drugs (NSAIDs) using Polypropylene Oxide Core PAMAM Dendrimer, *Int. J. Pharm.*, 2013, **451**, 18–22.
7 X. Shi, I. Bányai, M. T. Islam, W. Lesniak, D. Z. Davis, J. R. Baker Jr and L. Balogh, Generational, skeletal and substitutional diversities in generation one poly(amidoamine) dendrimer, *Polymer*, 2005, **46**, 3022–3034.
8 I. Bányai, M. Kéri, Z. Nagy, M. Berka and L. P. Balogh, Self-diffusion of water and poly(amidoamine) dendrimer in dilute aqueous solutions, *Soft Matter*, 2013, **9**, 1645–1655.
9 J. Peterson, V. Allikmaa, J. Subbi, T. Pehk and M. Lopp, Structural deviations in poly(amidoamine) dendrimer:a MALDI-TOF MS analysis, *Eur. Polym. J.*, 2003, **39**, 33–42.
10 R. Müller, C. Laschober, W. W. Szymanski and G. Allmaier, Determination of molecular weight, particle size, and density of high number generation PAMAM dendrimer using MALDI-TOF-MS and nES-GEMMA, *Macromolecules*, 2007, **40**, 5599–5605.
11 X. Shi, A. K. Patri, W. Lesniak, M. T. Islam, C. X. Zhang, J. R. Baker Jr and L. P. Balogh, Analysis of poly(amidoamine)-succinamic acid dendrimer by slab-gel electrophoresis and capillary zone electrophoresis, *Electrophoresis*, 2005, **26**, 2960–2967.

12 X. Shi, W. Lesniak, M. T. Islam, M. C. MuÑiz, L. P. Balogh and J. R. Baker Jr, Comprehensive characterization of surface-functionalized poly(amidoamine) dendrimer with acetamide, hydroxyl, and carboxyl groups, *Colloids Surf., A*, 2006, **272**, 139–150.

13 X. Shi, I. Majoros, A. K. Patri, X. Bi, M. T. Islam, A. Desai, T. R. Ganser and J. R. Baker Jr, Molecular heterogeneity analysis of poly(amidoamine) dendrimer-based mono- and multifunctional nanodevices by capillary electrophoresis, *Analyst*, 2006, **131**, 374–381.

14 H. M. Brothers, L. T. Piehler and D. A. Tomalia, Slab-gel and capillary electrophoretic characterization of polyamidoamine dendrimer, *J. Chromatogr. A*, 1998, **814**, 233–246.

15 A. Ebber, M. Vaher, J. Peterson and M. Lopp, Application of capillary zone electrophoresis to the separation and characterization of poly(amidoamine) dendrimer with an ethylenediamine core, *J. Chromatogr. A*, 2002, **949**, 351–358.

16 M. T. Islam, X. Shi, L. Balogh and J. R. Baker Jr, HPLC separation of different generations of poly(amidoamine) dendrimer modified with various terminal groups, *Anal. Chem.*, 2005, **77**, 2063–2070.

17 M. T. Islam, I. J. Majoros and J. R. Baker Jr, HPLC analysis of PAMAM dendrimer based multifunctional devices, *J. Chromatogr. B: Anal. Technol. Biomed. Life Sci.*, 2005, **822**, 21–26.

18 X. Shi, X. D. Bi and T. Rose Ganser, HPLC analysis of functionalized poly(amidoamine) dendrimer and the interaction between a folate–dendrimer conjugate and folate binding protein, *Analyst*, 2006, **131**, 842–848.

19 M. T. Islam, X. Shi, L. Balogh and J. R. Baker Jr, HPLC Separation of Different Generations of Poly(amidoamine) Dendrimer Modified with Various Terminal Groups, *Anal. Chem.*, 2005, **77**, 2063–2070.

20 C. A. Cason, S. A. Oehrle and T. A. Fabré, Improved Methodology for Monitoring Poly(amidoamine) Dendrimer Surface Transformations and Product Quality by Ultra Performance Liquid Chromatography, *J. Nanomater.*, 2008, **32**, 1–7.

